A Molecular-orbital Study of Tricarbonyl(1—5-η-cycloheptadienylium)iron and Tricarbonyl(1—5-η-cyclo-octadienylium)iron[†]

David A. Brown,* Noel J. Fitzpatrick, and Michael A. McGinn
Department of Chemistry, University College, Belfield, Dublin 4, Ireland

The self-consistent charge and configuration (SCCC) molecular-orbital method has been used to examine the electronic structures of the cyclodienyl complexes $[Fe(C_7H_9)(CO)_3]^+$ and $[Fe(C_8H_{11})(CO)_3]^+$. The geometrical conformations adopted by the rings and the barriers to $Fe(CO)_3$ rotation have been calculated and compared with those of $[Fe(C_5H_5)(CO)_3]^+$ and $[Fe(C_6H_7)(CO)_3]^+$. It was found that distortions of the dienyl π molecular orbitals introduced by the saturated part of the ring are critical to the structure adopted. Both the complexes prefer geometries in which the rings are non-planar: in a non-symmetrical conformation in the case of $[Fe(C_7H_9)(CO)_3]^+$, in which the hydrogen atoms of the C_2H_4 moiety are almost staggered with respect to one another and the $Fe(CO)_3$ group rotated by *ca.* 10° out of the 'mirror plane' of the complex; and a 'boat' geometry in the case of $[Fe(C_8H_{11})(CO)_3]^+$, once again displaying a staggered arrangement of the methylene hydrogen atoms. These predictions are in agreement with known structural data. Interconversion processes between conformational isomers are examined.

Complexes involving 1—5-η co-ordination of a cyclodienyl ligand to a transition metal-bearing fragment are well known.[1] The cyclopentadienyl group, unique in organometallic chemistry, may be regarded as the first member of a series of 1—5-η ligands (**1**)—(**4**), which are derived from it by successive insertions of methylene groups.

Although the number of reported complexes decreases markedly as ring size increases from five to eight carbon atoms, the cyclohexa-,[2,3] cyclohepta-,[4,5] and cyclo-octadienyl[6,7] systems have become a focus of interest due to the great stereo- and regio-selectivity of their reactions with nucleophiles, which suggests easy routes to specifically functionalised hydrocarbon molecules.[5,8]

However, despite the accumulation of a wealth of data, the factors influencing the site of nucleophilic addition have not been fully elucidated. The absence of any substituents on the co-ordinated dienyl generally results in the formation of 5-*exo* ring adducts.[9–13] Theoretical studies of cyclohexadienyl complexes have rationalised this behaviour in terms of the 'free valence' of the carbon atoms of the 1—5-η system. Pearson and co-workers[14] have proposed that this is closely linked to conformational effects in the ring; for example, a metal slippage resulting in partial de-co-ordination of one or more carbon atoms, leaving them susceptible to attack. This idea may also be used to explain the observed addition pattern in substituted cyclohexadienyls.

For complexes of the cycloheptadienyl ligand, however, evidence has been reported for intermediates resulting from initial attack at the metal atom of azide, ethoxide, and tri-n-butyl- and triethyl-phosphine,[15] and intermediates resulting from attack at the carbonyl-carbon atom by alkoxides have actually been isolated.[16] Further, in several related cases, where the final product is the thermodynamically stable ring adduct, experimental[17–19] and theoretical[20–24] evidence exists for intermediates involving initial metal attack. This suggests that the existence of such intermediates is a more general phenomenon than was once thought and even in cases where they have not yet been observed their occurrence cannot be ruled out.

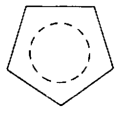
(1)

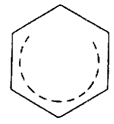
(2)

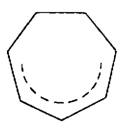
(3)

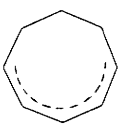
(4)

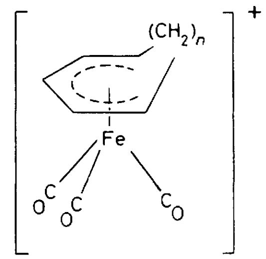

(5) *n* = 2 or 3

It is clear that the geometry adopted by these complexes is quite crucial to a discussion of their reactivity, and a conformational analysis has been carried out for various cyclohexadienyl ML_n complexes by several groups.[14,25,26]

In this paper, a detailed study of the conformations and electronic structures of tricarbonyl(1—5-η-cycloheptadienylium)iron and tricarbonyl(1—5-η-cyclo-octadienylium)iron (**5**) is presented. The reactivity of these species towards nucleophilic attack is the subject of a separate paper.[23]

Structural Information

Structural studies of 1—5-η-cycloheptadienyl and -cyclo-octadienyl complexes show, analogous to the cyclohexadienyl

---

[†] *Non-S.I. unit employed:* eV ≈ 1.60×10^{-19} J.

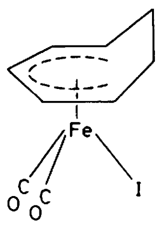

(6)

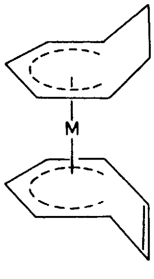

(7) M = Fe or Ru

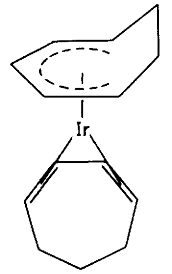

(8)

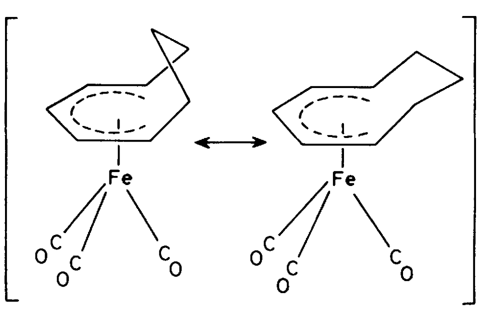

(10)

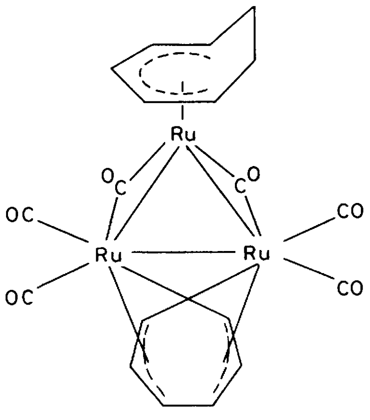

(9)

case,[27] distortions of the saturated part of the ring out of the 1—5-η plane, away from the metal atom. In addition, rotation about the C–C bonds within the $(CH_2)_n$ system permits further conformational freedom.

For cycloheptadienyl complexes, such rotations give rise to conformations of the ethane-type fragment ranging between fully eclipsed and fully staggered. The complexes whose structures are known lie between these extremes. In $[Fe(\eta^5\text{-}C_7H_9)(CO)_2I]$ (**6**) the angle between the 1—5-η plane and the best least-squares plane formed by C(5)C(6)C(7)C(1) is 144.5° and the C(5)C(6)C(7)C(1) dihedral angle is 23°.[28] For $[Ru(\eta^5\text{-}C_7H_7)(\eta^5\text{-}C_7H_9)]$ (**7**) the out-of-plane bend is 132° with a dihedral angle of 33°.[29] The analogous iron complex shows a similar structure.[30] The reported structure of $[Ir(\eta^5\text{-}C_7H_9)(\eta^4\text{-}C_7H_{10})]$ (**8**) shows an out-of-plane bend of 133° and a dihedral angle of 25°,[31] while the recently prepared $[Mn\{\eta^5\text{-}C_7H_8(PPh_3)\}(CO)_3]^+$ exhibits an out-of-plane bend of 135° and a dihedral angle of 11°.[32] The $(\eta^5\text{-}C_7H_9)M$ system has also been observed in $[Ru\{\eta^5\text{-}C_7H_7(SiMe_3)(C_6F_5)\}(CO)_2(SiMe_3)]$ (dihedral angle 37°),[33] and in $[Ru_3(C_7H_6)(\eta^5\text{-}C_7H_9)(CO)_6]$ (**9**), where it also exhibits an out-of-plane bend.[34] Finally, a number of other structures containing 1—5-η-bonded cycloheptadienyls are known, in which the aliphatic part of the ring is constrained to adopt an eclipsed conformation by incorporation into a second ring, *e.g.* *trans*-$[Mn_2(\eta\text{-}C_{10}H_8)(CO)_6]$.[35]

In the cyclo-octadienyl case, geometries involving both eclipsed and staggered conformations around the C–C bonds are included in the pathway represented by a 'flip' from a boat to a chair and *vice versa*, (**10**). All the known structures confirm a preference for the boat geometry; *e.g.* $[Zr(\eta^5\text{-}C_8H_{11})(dmpe)_2]$ (**11**) (dmpe = $Me_2PCH_2CH_2PMe_2$),[36] and in $[Cr(\eta^5\text{-}C_8H_{11})H(PF_3)_3]$ (**12**),[37] which may also be considered an agostic system,[38] where the out-of-plane angle is 123°.

In fact, the boat geometry is also adopted by 1—3-η-bonded

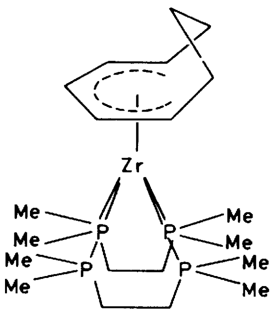

(11)

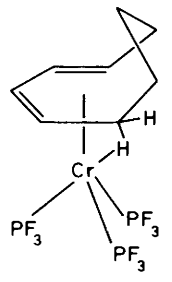

(12)

eight-membered rings, as in, for example, $[Fe(C_8H_{13})\{P(OMe)_3\}_3]^+$,[39] and recent n.m.r. evidence also suggests a boat conformation for 1—4-η-bound seven-membered rings, as in $[Fe(\eta^4\text{-}C_7H_{10})(CO)_2\{P(OMe)_3\}]$.[5]

Results and Discussion

Computational Method and Model Geometries.—Molecular-orbital (m.o.) calculations were performed using the self-consistent charge and configuration (SCCC) extended-Hückel method throughout, with the FORTICON8 computer program.[40—42] The basis functions for the iron atom comprised valence Slater-type 3*d*, 4*s*, and 4*p* atomic orbitals; 2*s* and 2*p* functions were included on the carbon and oxygen atoms and 1*s* on the hydrogens. The radial wavefunctions computed by Fitzpatrick and Murphy[43] as a least-squares fit to the self-consistent field (SCF) functions of Herman and Skillman[44] were chosen. Double-zeta orbitals were used for the *d* functions. A value of 1.3 was chosen as the exponent for the hydrogen atoms.

Valence-orbital ionisation potentials for nine configurations of the iron atom and two for carbon and oxygen were taken from the work of Basch *et al.*[45] as approximations to the diagonal terms of the coulomb matrix. Off-diagonal coulomb elements were calculated using the 'weighted' Wolfsberg–Helmholz formula, with $k = 1.75$.[46] These parameters have been summarised previously.[38] Calculations typically required 5—10 min of computing time (depending on the molecular size and rate of convergence) using an AMDAHL V8 computer with a VM/CMS operating system. In most cases, approximately 50 iterations were required to reach self-consistency. Based on the known *X*-ray structures of cycloheptadienyl and cyclo-octadienyl complexes, idealised model geometries were constructed for use in the calculations. Details of the bond lengths and angles used in these models are given in Figure 1.

Electronic Structure of the 1—5-η-*Dienyl Complexes.*—Before examining the electronic structure of the complexes in

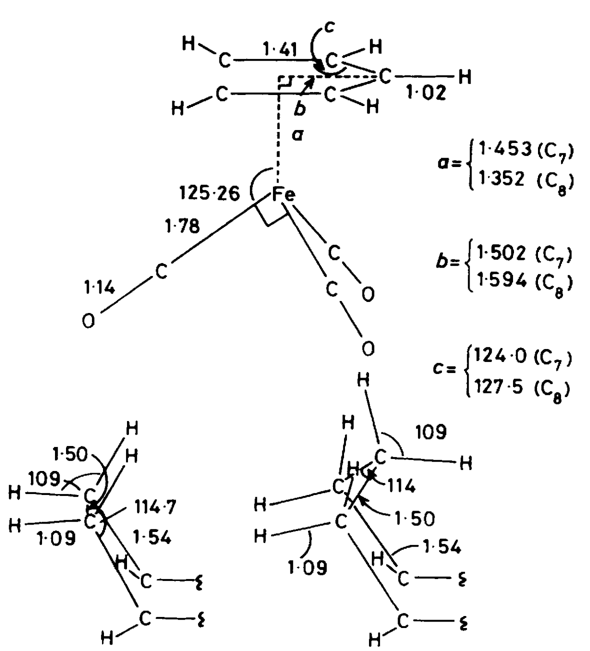

Figure 1. Model geometries (distances in Å, angles in °) used for calculations on $[Fe(C_7H_9)(CO)_3]^+$ and $[Fe(C_8H_{11})(CO)_3]^+$

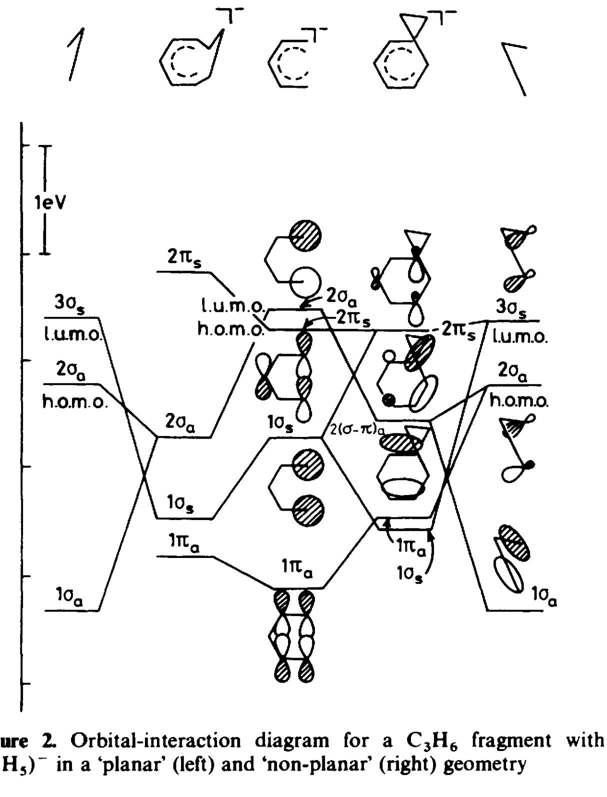

Figure 2. Orbital-interaction diagram for a C_3H_6 fragment with $(C_5H_5)^-$ in a 'planar' (left) and 'non-planar' (right) geometry

detail, the ring and $Fe(CO)_3$ fragments will be considered. The shapes and symmetries of the metal-bearing fragment m.o.s are well known,[47] but some discussion of the dienyl orbitals is relevant. Hoffmann and co-workers[25,47] have analysed the bonding in acyclic $[M(dienyl)L_3]$ complexes, in which the hydrocarbon fragment π frontier m.o.s are of 's' and 'a' symmetry. In heptadienyl and octadienyl rings, the saturated carbon group lying out of the 1—5-η plane causes a perturbation of these m.o.s, which affects their bonding capabilities with the $M(CO)_3$ group. This is illustrated by the fragment m.o. analysis of the bonding in C_8H_{11} (Figure 2).

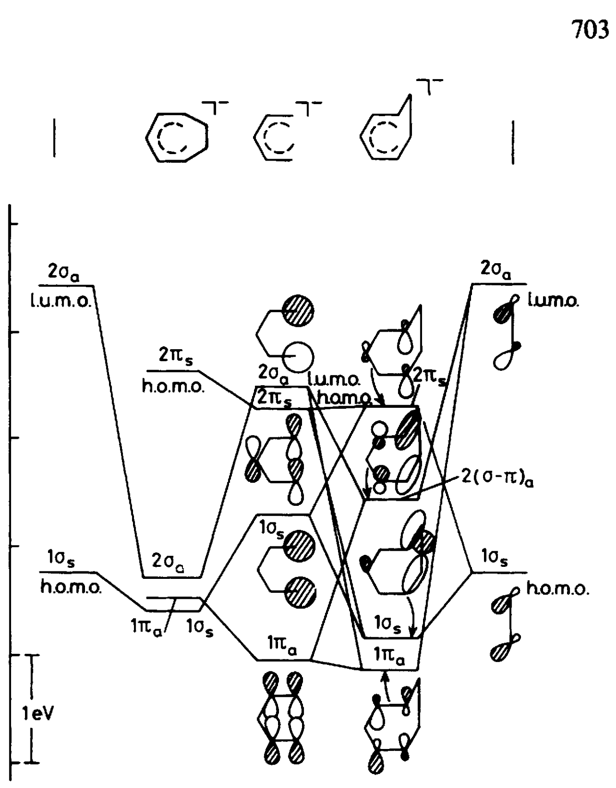

Figure 3. Orbital-interaction diagram for a C_2H_4 fragment with $(C_5H_5)^-$ in a 'planar' (left) and 'non-planar' (right) geometry

With the C_3H_6 fragment orientated so that its terminal carbon atoms lie coplanar with the dienyl fragment, the $2\pi_s$ and $1\pi_a$ dienyl m.o.s remain undistorted because the frontier m.o.s of the saturated fragment possess σ symmetry in the ring plane and thus do not overlap. As the C_3H_6 group is raised out of the plane, however, the overlap becomes non-zero and the σ-type frontier m.o.s interact with the π-$(C_5H_5)^-$ levels and the σ-type dienyl m.o.s mix into this interaction. This mixing 'weights' the orbitals either above or below the 1—5-η plane, and either towards or away from the 'open' end of the dienyl. These effects are also observed in the interaction of $(C_5H_5)^-$ and C_2H_4 to form the cycloheptadienyl ring (Figure 3), but their magnitude is not as great because the energy separations between the 'a' and 's' orbitals of the fragments are much greater. For example, the $1\pi_a$ orbital retains some electron density below the ring plane, located away from the open end of the dienyl.

We now turn to the complexes. Energy-level diagrams for tricarbonyl(1—5-η-cycloheptadienylium)iron and tricarbonyl-(1—5-η-cyclo-octadienylium)iron are compared in Figure 4. The levels are drawn so as to show their parentage in the m.o.s of the ring and $Fe(CO)_3$ fragments. It is found that the energy levels of the complex differ appreciably from those of the fragments only in the h.o.m.o.-l.u.m.o. region, hence only these have been drawn (h.o.m.o. = highest occupied molecular orbital, l.u.m.o. = lowest unoccupied molecular orbital). Important levels are labelled 's' or 'a' according to whether they are symmetric or antisymmetric with respect to the mirror plane of the entire complex. The diagram shows that the interaction of the frontier m.o.s is weaker in the case of the octadienyl complex, resulting in poorer stabilisations.

In both complexes, the major interactions occur between the $2\pi_s$, $2\sigma_a$, and $1\pi_a$ m.o.s on the ring and the $2e_{a,s}$ l.u.m.o. of the

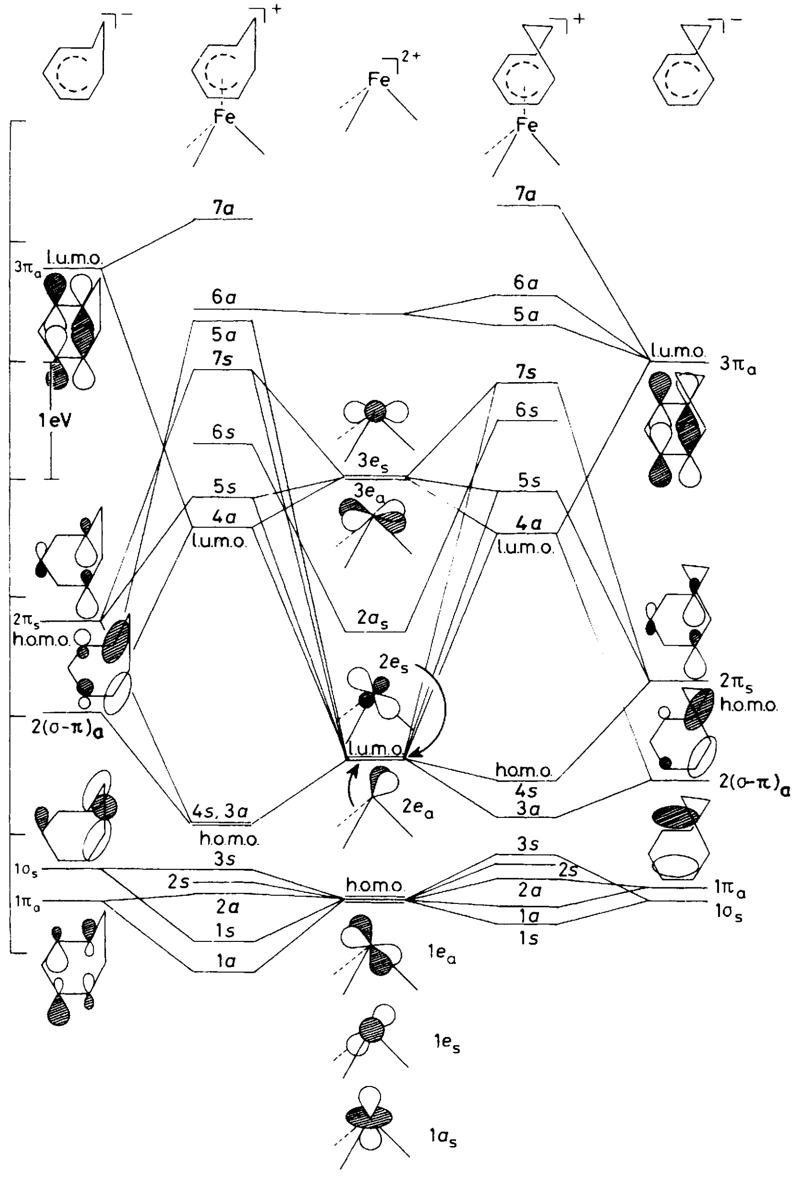

Figure 4. Orbital-interaction diagram for $(C_7H_9)^-$ (left) and $(C_8H_{11})^-$ (right) with $Fe(CO)_3^{2+}$ to yield $[Fe(C_7H_9)(CO)_3]^+$ and $[Fe(C_8H_{11})(CO)_3]^+$

$Fe(CO)_3$ group. The $1e_{a,s}$ levels act largely as 'lone pairs,' but also mix into the $2e$ interactions in an antibonding sense. The $1\pi_s$ and $3\pi_s$ m.o.s on the ring lie respectively too low and too high in energy to interact effectively. On the other hand, the $2\pi_a$ m.o. interacts strongly with the $3e_a$ $Fe(CO)_3$ l.u.m.o. and makes a significant contribution to the l.u.m.o. group of the complex.

Conformation of the $M(CO)_3$ *Group and the Strength of the Metal–Ring Bond.*—The known structures of [M(cyclodienyl)-L_3] complexes indicate a preference for the 'staggered' geometry (**5**), in which one of the ligands lies beneath the 'open' end of the polyene.[27] This may be explained in terms of the overlaps between the $2\pi_s$ and $2e_s$,$1e_s$ fragment m.o.s (Table 1). The overlap between $2e_s$ and $2\pi_s$ decreases from the staggered to the eclipsed configuration, reducing the size of the bonding interaction and destabilising the h.o.m.o of the complex. This effect is reinforced by a decrease in the antibonding $1e_s$–$2\pi_s$ overlap from the eclipsed to the staggered configuration, as evidenced by a decrease in the corresponding group overlap integral.

The calculated energy barriers to carbonyl rotation in $[Fe(C_5H_5)(CO)_3]^+$, $[Fe(C_6H_7)(CO)_3]^+$, $[Fe(C_7H_9)(CO)_3]^+$, and $[Fe(C_8H_{11})(CO)_3]^+$ are shown in Figure 5. Although the height of the barriers is overestimated, a clear pattern of increasing barrier height with increasing ring size emerges. The barrier is zero in the case of $[Fe(C_5H_5)(CO)_3]^+$ because the ring possesses two mirror planes. This change in barrier size is obviously controlled by the strength of the metal–ring bonding, which in turn is influenced both by the geometry of the ring and the electronic effects of the aliphatic portion of the ring. In order to bridge the expanding size of this group as the ring size increases, the dienyl opens out. This effectively reduces the overlap between the ring and any metal fragment orbitals which are weighted towards the 'open' end; *e.g.* $2\pi_s$–$2e_s$ and $1\pi_a$–$2e_a$ in the staggered conformer and $1\pi_a$–$1e_a$ in the eclipsed one. The effect of such a reduction on the barrier heights of three pentadienyl complexes in which the dienyl ligand is taken from the six-, seven-, and eight-membered cyclodienyl ligands is shown in Table 2. The size of the barrier decreases from

Table 1. Overlap integrals and rotational barriers for tricarbonyl(1—5-η-cyclodienylium)iron complexes

Complex	Overlap integral				Rotational barrier (eV)
	$\langle 2\pi_s \vert 2e_s\rangle$	$\langle 2\pi_s \vert 1e_s\rangle$	$\langle 1\pi_a \vert 2e_a\rangle$	$\langle 1\pi_a \vert 1e_a\rangle$	
$[Fe(C_6H_7)(CO)_3]^+$					
staggered	0.1585	0.0107	0.1361	0.0210	1.7
eclipsed	0.1355	0.0864	0.1262	0.0451	
$[Fe(C_7H_9)(CO)_3]^+$					
staggered	0.1757	0.0031	0.1163	0.0167	2.1
eclipsed	0.1558	0.0832	0.1104	0.0344	
$[Fe(C_8H_{11})(CO)_3]^+$					
staggered	0.1587	0.0216	0.1011	0.0179	2.4
eclipsed	0.1311	0.0911	0.0973	0.0313	

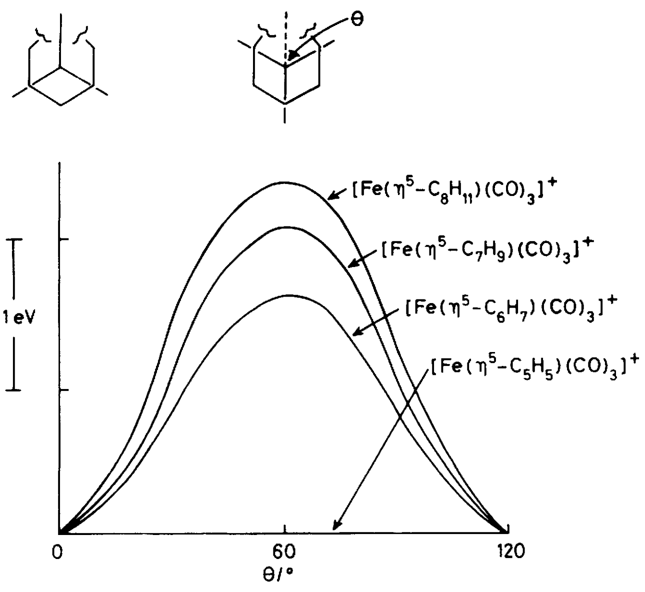

Figure 5. Energy profile for rotation of the $M(CO)_3$ group relative to the ring in each cyclodienyl complex

$[Fe(C_6H_7)(CO)_3]^+$ to $[Fe(C_8H_{11})(CO)_3]^+$, opposite to the trend observed with the cyclic ligands.

The reversal of this order is due to the distortion of the frontier m.o.s discussed earlier. In the cycloheptadienyl and cyclo-octadienyl cases, the shift of electron density towards C(1) and C(5) in the case of the $2\pi_s$ orbital stabilises the staggered configuration relative to the eclipsed, due to an increase in the $2e_s$–$2\pi_s$ bonding overlap. The overlaps show that this effect is most pronounced for the seven-membered ring, because the distortion which favours the staggered geometry is larger than in $[Fe(C_6H_7)(CO)_3]^+$, but the ring has not opened out sufficiently to cancel the effect, as it has in tricarbonyl(1—5-η-cyclo-octadienylium)iron.

In the cycloheptadienyl case the $1\pi_a$ level is polarised towards the closed end of the dienyl group, and this improves overlap with the $2e_a$ $M(CO)_3$ m.o.s in the 'eclipsed' configuration, counterbalancing the effects on the 'staggered' geometry. This does not occur for the octadienyl because there the $1\pi_a$ level has a very poor interaction with the metal, due to the attenuation of its 'below-plane' electron density.

To summarise, the observed ordering of the barrier heights is a result of the operation of several factors. In the acyclic tricarbonyl(pentadienylium)iron complexes, the barrier height decreases as the polyene opens out because the bonding overlaps (*e.g.* $\langle 2\pi_s|2e_s\rangle$, $\langle 1\pi_a|2e_a\rangle$) between the fragments are reduced and the antibonding ones are improved ($\langle 2\pi_s|1e_s\rangle$). The introduction of an out-of-plane CH_2 group attenuates the below-plane extent of the π frontier m.o.s and weakens the metal–ring bonding in both the eclipsed and staggered conformations, reducing the barrier height. As the aliphatic group grows in size, it perturbs the ring m.o.s, creating a σ–π hybrid which is polarised towards C(1) and C(5), cancelling the effect of the opening out of the dienyl, and improving metal–ring bonding, increasing the barrier height again.

Conformation of the Cyclodienyl Ligands.—Hoffmann and Hofmann[25] demonstrated that the observed non-planarity of the ring in $[Fe(C_6H_7)(CO)_3]^+$ is electronic in origin, traceable to a repulsive interaction between the $2e_s$ l.u.m.o. of the ML_3 fragment and the contribution from the methylene-hydrogen atoms in the $2\pi_s$ ring h.o.m.o.

We have studied this phenomenon for the seven- and eight-membered analogues, concentrating on two types of conformational change: (*a*) out-of-plane bending of the aliphatic part of the ring (with and without 'relaxation', *i.e.* bending below the 1—5-η-carbon plane) of the 'terminal' dienyl hydrogen atoms, H(1) and H(5); (*b*) changes within the aliphatic fragment due to rotation around the C–C bonds.

Co-ordinate system. The co-ordinates used in this study are depicted in Figure 6. For the cycloheptadienyl case, the out-of-plane bend is defined by α [Figure 6(*a*)], the angle described by line segments joining the 'centre' of the dienyl (O) to the midpoint (A) of C(1) ⋯ C(5) and from A to the midpoint (B) of C(6)–C(7). Variation of the conformation of the C_2H_4 group from eclipsed to staggered is achieved by rotating the C(6)–C(7) bond about the AB axis, like a propeller (through an angle β), while at the same time adjusting the AB distance (X) to keep the C(5)–C(6) and C(7)–C(1) distances fixed. Atoms H(6A) and H(6B), H(7A) and H(7B) automatically adopt the correct conformation during such a rotation by being constrained to remain in planes perpendicular to the C(5)C(6)C(7) and C(6)C(7)C(1) planes respectively, each of which bisect the C(5)C(6)C(7) and C(6)C(7)C(1) angles. The out-of-plane bending motion is simulated by varying α, and it is possible to introduce a 'relaxation' process for H(1) and H(5), whereby they are constrained to lie in the C(2)C(1)C(7) and C(4)C(5)C(6) planes, thus dropping below the 1—5-η plane as bending occurs.

In a similar way the conformations in the cyclo-octadienyl ligand can be described by two co-ordinates: α, the out-of-plane bending angle, and β, the ABC(7) angle. Variation of β with a relaxation pathway for H(6A),H(6B) and H(8A),H(8B)

Table 2. Overlap integrals and rotational barriers for tricarbonyl(1—5-η-pentadienylium)iron complexes

'Parent' complex	Overlap integral				Rotational barrier (eV)
	$\langle 2\pi_s\|2e_s\rangle$	$\langle 2\pi_s\|1e_s\rangle$	$\langle 1\pi_a\|2e_a\rangle$	$\langle 1\pi_a\|1e_a\rangle$	
$[Fe(C_6H_7)(CO)_3]^+$					
staggered	0.1690	0.0112	0.2040	0.0537	2.3
eclipsed	0.1456	0.0895	0.2063	0.0426	
$[Fe(C_7H_9)(CO)_3]^+$					
staggered	0.1502	0.0342	0.1978	0.0565	1.7
eclipsed	0.1165	0.0987	0.2053	0.0254	
$[Fe(C_8H_{11})(CO)_3]^+$					
staggered	0.1315	0.0597	0.1860	0.0581	0.6
eclipsed	0.0886	0.1056	0.1988	0.0048	

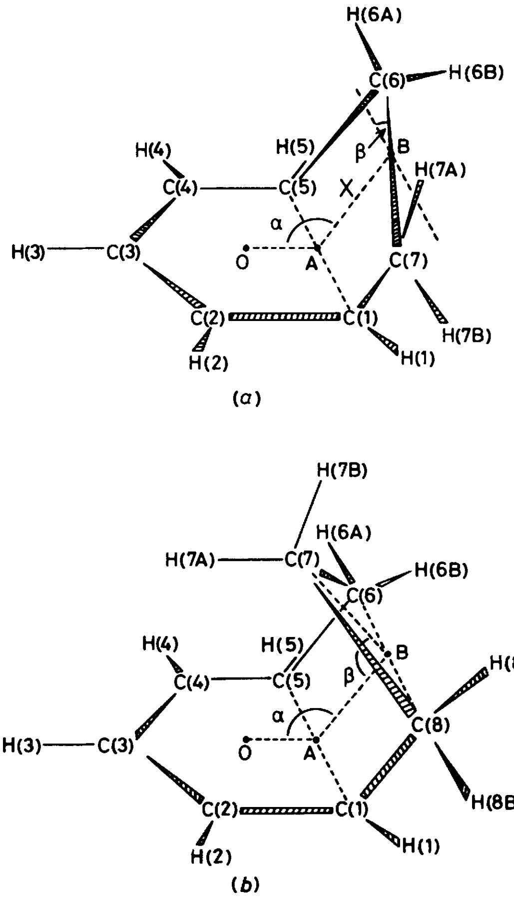

Figure 6. Definition of the geometrical co-ordinates α and β used to describe the ring conformations in (*a*) tricarbonyl(1—5-η-cyclohepta-dienylium)iron and (*b*) tricarbonyl(1—5-η-cyclo-octadienylium)iron

analogous to that used for the seven-membered ring allows geometries ranging from the boat (β < 180°) to the chair (β > 180°) to be generated. In the chair and boat geometries the methylene-hydrogen atoms are staggered, but in the intermediate β = 180° geometry with C(5), C(6), C(7), C(8), and C(1) coplanar they are eclipsed. Calculations of the total energies of the isolated rings *versus* variations in both α and β show that both the isolated cycloheptadienyl and cyclo-octadienyl rings adopt geometries in which the aliphatic hydrogen atoms are staggered, with β *ca.* 20° in tricarbonyl-(1—5-η-cycloheptadienylium)iron and 126° in tricarbonyl-(1—5-η-cyclo-octadienylium)iron. However, whereas the isolated cycloheptadienyl prefers a planar geometry (α = 180°), the cyclo-octadienyl ring adopts a boat geometry with α = 145°. These geometries may be explained by considering the energies of the frontier ring m.o.s on bending. For α > 120°, the $2\pi_s$ h.o.m.o. remains constant in energy, indicating that the conclusions drawn will be independent of whether the rings are positively or negatively charged or neutral.

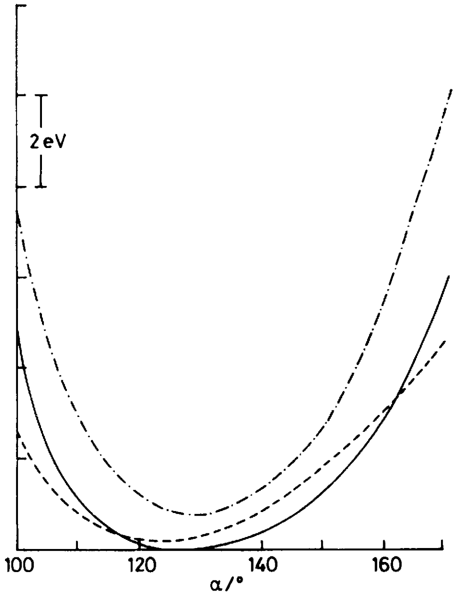

Figure 7. Total energy of $[Fe(C_7H_9)(CO)_3]^+$ in the eclipsed (– – –, β = 0°), partially staggered (——, β = 20.0°), and fully staggered (— · —, β = 24.87°) conformations *versus* out-of-plane bending angle, α

The cycloheptadienyl ring adopts the planar geometry because the $(\sigma-\pi)_a$ hybrid h.o.m.o. (Figure 2) favours this arrangement, repulsions between C(2) and C(4), and C(6) and C(7) developing on bending. In C_8H_{11} this effect is swamped by the favourable C(7)–C(3) overlap in the boat conformer, which is spread over all the h.o.m.o.s. If this is disrupted as in the chair conformer, then planarity is preferred.

Complexes. The main conformational energetics may be represented as a surface in the αβ domain. The surface for $[Fe(C_7H_9)(CO)_3]^+$ is illustrated in Figure 7. At all values of β the ring is predicted to possess a non-planarity analogous to

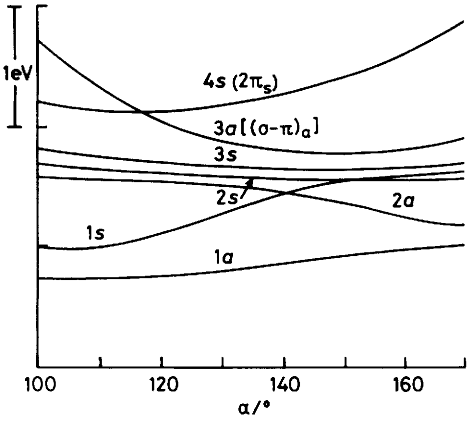

Figure 8. Energies of the frontier m.o.s of eclipsed $[Fe(C_7H_9)(CO)_3]^+$ *versus* out-of-plane bending angle, α

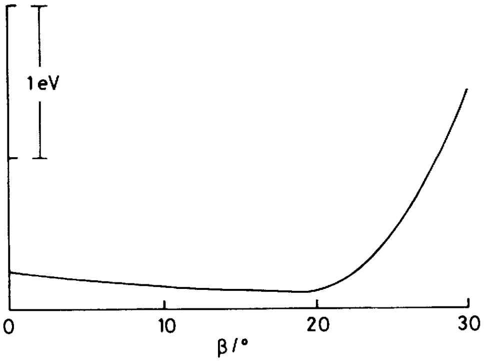

Figure 9. Total energy of $[Fe(C_7H_9)(CO)_3]^+$ as a function of β at α = 124°

that observed for $[Fe(C_6H_7)(CO)_3]^+$, traceable to the energy profiles of the $2\pi_s$ (4*s*) and $(\sigma-\pi)_a$ (3*a*) hybrid h.o.m.o.s of the complex (Figure 8). As in the isolated ring, the $(\sigma-\pi)_a$ m.o. favours a planar geometry, while the $2\pi_s$ prefers a bent one due to repulsion between the metal $2e_s$ orbital and the contributions from H(6A) and H(7A). The result is the observed minimum at α *ca.* 124°, smaller than that experimentally observed for C_7H_9 complexes. Moving along the β co-ordinate at this value of α, along the bottom of a 'valley,' we find that, as in the isolated ring, a minimum is found to occur at β *ca.* 20° (Figure 9). This represents the best compromise between straining the ring as the ethane group tries to become totally staggered and the repulsions between the hydrogen atoms that occur in the fully eclipsed case.

The most important consequence of this staggering of the saturated fragment is that it introduces an asymmetry into the complex. Further, H(6A) is brought very close to the metal atom, and to minimise the repulsion in the $2\pi_s$ ring h.o.m.o. the $M(CO)_3$ fragment rotates slightly, further enhancing the asymmetry. Our calculations estimate this rotation to be *ca.* 10°, though the energies involved are very small. This is encouraging because it is precisely what is observed for $[Fe(\eta^5\text{-}C_7H_9)(CO)_2I]$.[28]

Energy profiles for ring bending in the chair and boat conformers of $[Fe(C_8H_{11})(CO)_3]^+$ are given in Figure 10. The boat is predicted to be the most stable conformation, with α *ca.* 120°, smaller than that observed for the isolated ring. The chair conformation is of higher energy, due to the loss of the favourable C(7)–C(3) interaction, but still exhibits an out-of-plane bend because of the repulsion between C(7)H(7A,B) and the metal. Along the β co-ordinate, the boat and chair conformers are represented by two local minima separated by a transition state in which the C(1)C(8)C(7)C(6)C(5) group is planar (Figure 11), with approximately 1.5 eV required to flip from boat to chair and 0.8 eV for the reverse process. Once again the origins of the out-of-plane bend can be traced to the behaviour of the frontier h.o.m.o.s of the complex.

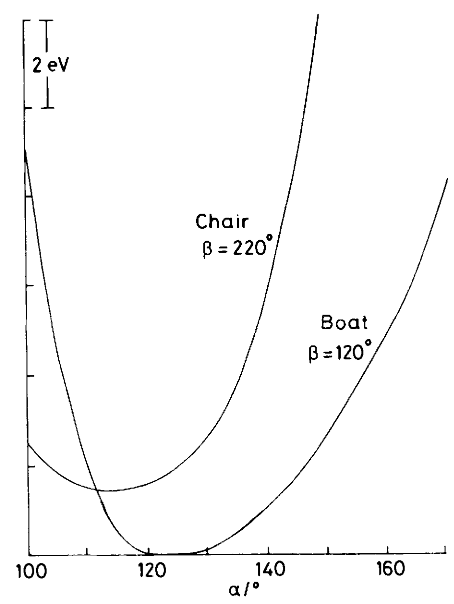

Figure 10. Total energy of $[Fe(C_8H_{11})(CO)_3]^+$ *versus* angle α for the 'chair' and 'boat' conformations

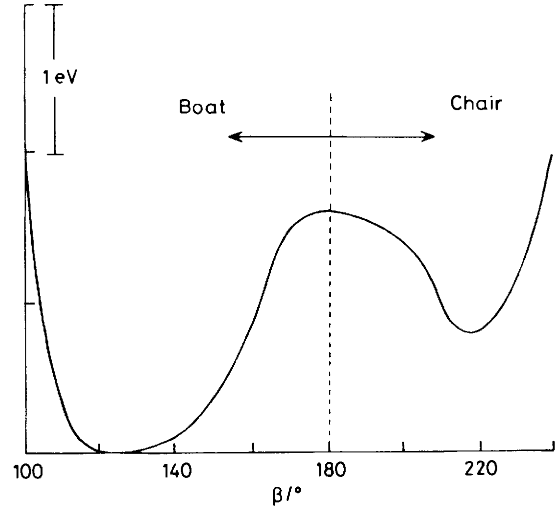

Figure 11. Total energy of $[Fe(C_8H_{11})(CO)_3]^+$ as a function of β showing two minima corresponding to the 'boat' and 'chair' conformations, at α = 120°

'Relaxation' of H(1) *and* H(5). During the out-of-plane bending motions described in the previous section, the 'terminal' dienyl hydrogen atoms, H(1) and H(5), were constrained to lie in the plane of C(1)—C(5). Calculations were also performed using a simple mechanism,[25] whereby H(1) and H(5) would be allowed to 'relax' out-of-plane during bending. The atoms were constrained to lie in the C(7)C(1)C(2) and C(4)C(5)C(6) planes respectively for the heptadienyl, and the C(8)C(1)C(2) and

C(4)C(5)C(6) planes respectively for the octadienyl. Analogous to the results of Hoffmann and Hofmann,[25] this relaxation was found to lead to destabilisation in all cases, both for isolated and complexed rings. The reason for this is that in the frontier complex m.o.s, *e.g.* *3a,s*, the contributions from H(1) and H(5) are of opposite phase to those of the C(1),C(5)–M($2e_{a,s}$) bond, and as these atoms are depressed below the plane they move closer to the metal, resulting in a repulsive interaction. Nevertheless, since the known structures do indicate a small out-of-plane distortion of H(1) and H(5), other factors must also operate.

Longitudinal and Lateral Displacement of the $M(CO)_3$ *Group Relative to the Ring.*—Energy profiles for displacement of the $Fe(CO)_3$ group relative to the ring, lateral displacement perpendicular to the mirror plane and longitudinal displacement within the mirror plane, were also calculated. For each complex a barrier exists to lateral displacement. Within the mirror plane, the metal occupies a position approximately equidistant from each 1—5-η carbon in $[Fe(C_7H_9)(CO)_3]^+$, but in $[Fe(C_8H_{11})(CO)_3]^+$ it is predicted to lie closer to C(2)—C(4) than to C(1) and C(5).

Conclusions

This study shows that in both $[Fe(C_7H_9)(CO)_3]^+$ and $[Fe(C_8H_{11})(CO)_3]^+$ the ring assumes a non-planar geometry analogous to that observed in $[Fe(C_6H_7)(CO)_3]^+$, for similar reasons. This non-planarity gives rise to a perturbation of the ring frontier m.o.s and, in particular, introduces a σ–π hybrid antisymmetric m.o. which is important in determining the strength of the metal–ring bonding. The distortion of the frontier ring m.o.s towards C(1) and C(5), combined with the opening out of the dienyl fragment to bridge the larger aliphatic group, is responsible for the predicted increase in the barrier to $Fe(CO)_3$ rotation with increasing ring size, the staggered geometry being preferred in all cases. Both complexes adopt geometries in which the hydrogen atoms on the aliphatic part of the ring are as staggered as possible within the constraints imposed by the 1—5-η moiety. In tricarbonyl(1—5-η-cyclooctadienylium)iron this produces a boat rather than a chair geometry, due to the added bonding interaction between C(3) and C(7) which the former allows. In tricarbonyl(1—5-η-cycloheptadienylium)iron the staggered C_2H_4 moiety introduces an asymmetry into the ring. Both of these effects are confirmed by *X*-ray determinations of the ring structures.

References

1 F. A. Cotton and G. Wilkinson, 'Advanced Inorganic Chemistry,' 4th edn., Wiley, New York, 1980.
2 D. Jones, L. Pratt, and G. Wilkinson, *J. Chem. Soc.*, 1962, 4458.
3 E. O. Fischer and R. D. Fischer, *Angew. Chem.*, 1960, **72**, 919.
4 H. J. Dauben and D. J. Bertelli, *J. Am. Chem. Soc.*, 1961, **83**, 497, 5049.
5 A. J. Pearson, S. L. Kole, and T. Ray, *J. Am. Chem. Soc.*, 1984, **106**, 6060.
6 A. J. Deeming, S. S. Ullah, A. J. P. Domingos, B. F. G. Johnson, and J. Lewis, *J. Chem. Soc., Dalton Trans.*, 1974, 2093.
7 J. Evans, B. F. G. Johnson, and J. Lewis, *J. Chem. Soc., Dalton Trans.*, 1972, 2668.
8 A. J. Pearson and C. W. Ong, *J. Org. Chem.*, 1982, **47**, 3780.
9 M. A. Hashmi, J. D. Munro, P. L. Pauson, and J. M. Williamson, *J. Chem. Soc. A*, 1967, 240.
10 A. J. Birch, P. E. Cross, J. Lewis, D. White, and S. B. Wild, *J. Chem. Soc. A*, 1968, 332.
11 A. J. Birch, K. B. Chamberlin, M. A. Haas, and S. J. Thompson, *J. Chem. Soc., Perkin Trans. 1*, 1973, 1882.
12 G. R. John and L. A. P. Kane-Maguire, *J. Organomet. Chem.*, 1976, **120**, C45.
13 D. A. Brown, N. J. Fitzpatrick, W. K. Glass, and P. K. Sayal, *Organometallics*, 1984, **3**, 1137.
14 O. Eisenstein, W. Butler, and A. J. Pearson, *Organometallics*, 1984, **3**, 1150.
15 D. A. Brown, S. K. Chawla, and W. K. Glass, *Inorg. Chim. Acta*, 1976, **19**, L31.
16 D. A. Brown, W. K. Glass, and F. M. Hussein, *J. Organomet. Chem.*, 1980, **186**, C58.
17 R. H. Hooker and A. J. Rest, *J. Organomet. Chem.*, 1982, **234**, C23.
18 D. A. Brown, N. J. Fitzpatrick, W. K. Glass, and T. H. Taylor, *J. Organomet. Chem.*, 1984, **275**, C9.
19 D. A. Brown, N. J. Fitzpatrick, W. K. Glass, and T. H. Taylor, *Organometallics*, in the press.
20 D. A. Brown, J. P. Chester, and N. J. Fitzpatrick, *J. Organomet. Chem.*, 1978, **155**, C21.
21 D. A. Brown, J. P. Chester, and N. J. Fitzpatrick, *Inorg. Chem.*, 1982, **21**, 2723.
22 D. A. Brown, N. J. Fitzpatrick, and M. A. McGinn, *J. Organomet. Chem.*, 1984, **275**, C5.
23 D. A. Brown, N. J. Fitzpatrick, and M. A. McGinn, *J. Organomet. Chem.*, 1985, **293**, 235.
24 D. A. Brown, N. J. Fitzpatrick, M. A. McGinn, W. K. Glass, and T. H. Taylor, *Organometallics*, in the press.
25 R. Hoffmann and P. Hofmann, *J. Am. Chem. Soc.*, 1976, **98**, 598.
26 C. R. Nurse and D. M. P. Mingos, *J. Organomet. Chem.*, 1980, **184**, 281.
27 M. R. Churchill and F. R. Scholer, *Inorg. Chem.*, 1969, **8**, 1950.
28 D. A. Brown, D. Cunningham, W. K. Glass, and M. T. Ubeid, unpublished work.
29 H. Schmid and M. L. Ziegler, *Chem. Ber.*, 1976, **109**, 125.
30 J. R. Blackborow, K. Hildenbrand, E. A. K. von Gustorf, A. Scrivanti, C. R. Eady, and D. Ehnholt, *J. Chem. Soc., Chem. Commun.*, 1976, 16.
31 J. Müller, H. Menig, G. Huttner, and A. Frank, *J. Organomet. Chem.*, 1980, **185**, 251.
32 E. D. Hong, M. Quin-jin, W. T. Robinson, P. G. Willard, and D. A. Sweigart, *Organometallics*, 1985, **4**, 871.
33 J. A. K. Howard, S. A. R. Knox, V. Riera, B. A. Sosinsky, F. G. A. Stone, and P. Woodward, *J. Chem. Soc., Chem. Commun.*, 1974, 673.
34 R. Bau, J. C. Burt, S. A. R. Knox, R. M. Laine, R. P. Phillips, and F. G. A. Stone, *J. Chem. Soc., Chem. Commun.*, 1973, 726.
35 M. R. Churchill and P. H. Bird, *Inorg. Chem.*, 1968, **7**, 1793.
36 M. B. Fischer, E. J. James, T. J. McNeese, S. C. Nyburg, B. Posin, W. Wong-Ng, and S. S. Wreford, *J. Am. Chem. Soc.*, 1980, **102**, 4941.
37 J. R. Blackborow, C. R. Eady, F-W. Grevels, E. A. K. von Gustorf, A. Scrivanti, O. S. Wolfbeis, R. Benn, D. J. Brauer, C. Kruger, P. J. Roberts, and Y-H. Tsay, *J. Chem. Soc., Dalton Trans.*, 1981, 661.
38 N. J. Fitzpatrick and M. A. McGinn, *J. Chem. Soc., Dalton Trans.*, 1985, 1637.
39 R. K. Brown, J. M. Williams, A. J. Schultz, G. D. Stucky, S. D. Ittel, and R. L. Harlow, *J. Am. Chem. Soc.*, 1980, **102**, 981.
40 R. Hoffmann and W. N. Lipscomb, *J. Chem. Phys.*, 1962, **36**, 3179, 3489.
41 R. Hoffmann and W. N. Lipscomb, *J. Chem. Phys.*, 1962, **32**, 2872.
42 J. Howell, A. Rossi, D. Wallace, K. Haraki, and R. Hoffmann, FORTICON8, Quantum Chemistry Program Exchange, Program No. 344, 1977.
43 N. J. Fitzpatrick and G. H. Murphy, *Inorg. Chim. Acta*, 1984, **87**, 41.
44 F. Herman and S. Skillman, 'Atomic Structure Calculations,' Prentice-Hall, New Jersey, 1963.
45 H. Basch, A. Viste, and H. B. Gray, *Theor. Chim. Acta*, 1965, **3**, 463.
46 J. H. Ammeter, H-B. Bürgi, J. C. Thibeault, and R. Hoffmann, *J. Am. Chem. Soc.*, 1978, **100**, 3686.
47 T. A. Albright, P. Hofmann, and R. Hoffmann, *J. Am. Chem. Soc.*, 1977, **99**, 7546.

Received 21*st June* 1985; *Paper* 5/1047